

## Supporting Information

1

### 2 **1. Size distributions of as-prepared nanocomposites by dynamic light scattering** 3 **tests.**

4 As exhibited in Fig. S1, the above-mentioned three nanoprobe all had an average  
5 hydrodynamic size of less than 100 nm, which indicated that they were suitable for  
6 intracellular assays[1]. And PPy@RhB-PAA-FITC nanocomposites had an average  
7 hydrodynamic size of 99.9 nm, which was larger than TEM result due to the presence  
8 of PAA and PEI. And the PDI value of less than 0.2 indicated that PPy@RhB-PAA-  
9 FITC nanocomposites possessed good aqueous dispersity[2].

### 10 **2. FTIR**

11 FTIR was carried out to further study the chemical composition and structure of  
12 obtained nanocomposites. As shown in Fig. S4, the peaks at about 3420, 1547 and 1303  
13  $\text{cm}^{-1}$  for all nanocomposites were assigned to the stretching vibrations of N-H/O-H,  
14 C=C and C-N, respectively. The C-H bending vibration and =C-H in-plane vibration  
15 were associated with the bands at 1463 and 1037  $\text{cm}^{-1}$ , respectively. The C-H out-  
16 plane/in-plane deformation vibration peaks were found at 1176 and 907  $\text{cm}^{-1}$ ,  
17 respectively. The band of C=O stretching vibration was presented at 1636  $\text{cm}^{-1}$ .  
18 Furthermore, two peaks at 1696 and 1335  $\text{cm}^{-1}$  were appeared in PPy@RhB-PAA  
19 nanocomposites, which belonged to C=O stretching and C-H bending vibrations of PAA.  
20 Finally, polymer PEI was chosen as intermediate linker for connecting FITC to  
21 nanocomposites. The C-N and C=S vibration were observed at 1469 and 1183  $\text{cm}^{-1}$ ,  
22 respectively, because FITC was connected firstly with PEI via the reaction between  
23 isothiocyanate and carboxyl group. Then obtained PEI-FITC was linked with  
24 PPy@RhB-PAA nanocomposites through amide reaction, resulting the presence of C=O  
25 and N-H vibrations in PPy@RhB-PAA-FITC nanocomposites. Moreover, the -CH<sub>2</sub>-  
26 vibration was emerged at 1875  $\text{cm}^{-1}$  and N-H vibration was shifted to 3382  $\text{cm}^{-1}$  in the  
27 final harvested nanocomposites, which was due to the presence of PEI chains.  
28 Therefore, the FTIR data confirmed the successful construction of PPy@RhB-PAA-  
29 FITC nanocomposites.

### 1 3. Calculation of photothermal conversion efficiency

2 The photothermal conversion efficiency ( $\eta$ ) of nanocomposites was assessed  
3 following the Roper's method[3]. The details of calculation of photothermal conversion  
4 efficiency were as follows:

$$\eta = \frac{hA(\Delta T_{max,mix} - \Delta T_{max,H_2O})}{I(1 - 10^{-A_{808}})} \quad (1)$$

5  
6 where  $h$  is the heat transfer coefficient,  $A$  is the surface area of the container.  $\Delta T_{max,mix}$   
7 and  $\Delta T_{max,H_2O}$  are the temperature variations of nanocomposites solution and deionized  
8 water after laser radiation.  $I$  refers to the laser power and  $A_{808}$  is the absorbance of  
9 nanocomposites at 808 nm.

10 Then the value of  $hA$  was calculated from equation (2):

$$hA = \frac{m_{H_2O} C_{p,H_2O}}{\tau_s} \quad (2)$$

11  
12 where  $m_{H_2O}$  refer to the mass and heat capacity of deionized water, separately.  $\tau_s$  is a  
13 sample system time constant.

14 The value of  $\tau_s$  was obtained from equation (3) and (4):

$$\theta = \frac{(T - T_{surr})}{(T_{max} - T_{surr})} \quad (3)$$

$$t = -\tau_s \ln \theta \quad (4)$$

15  
16  
17 where  $\theta$  is a dimensionless parameter,  $T$  refers the temperature during natural cooling  
18 stage.  $T_{surr}$  is the environment temperature and  $T_{max}$  is the maximum steady  
19 temperature. Therefore,  $\tau_s$  is able to determine.

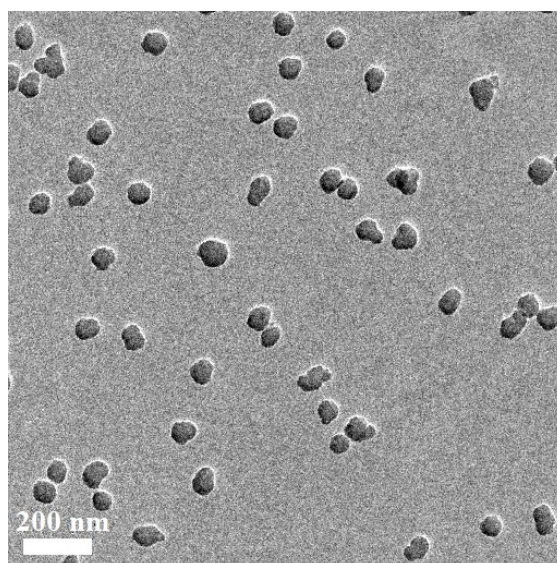
20 Finally, substituting the corresponding value into equation (1), the photothermal  
21 conversion efficiency ( $\eta$ ) of PPy@RhB-PAA-FITC nanocomposites was assessed to be  
22 36.24%.

23 [1] Y. Liu, P. Bhattarai, Z. Dai and X. Chen, Chem. Soc. Rev., 2019, 48, 2053-2108.

24 [2] M. Chen, X. Liu, A. Fahr, Int. J. Pharmaceut., 2011, 408, 223-234.

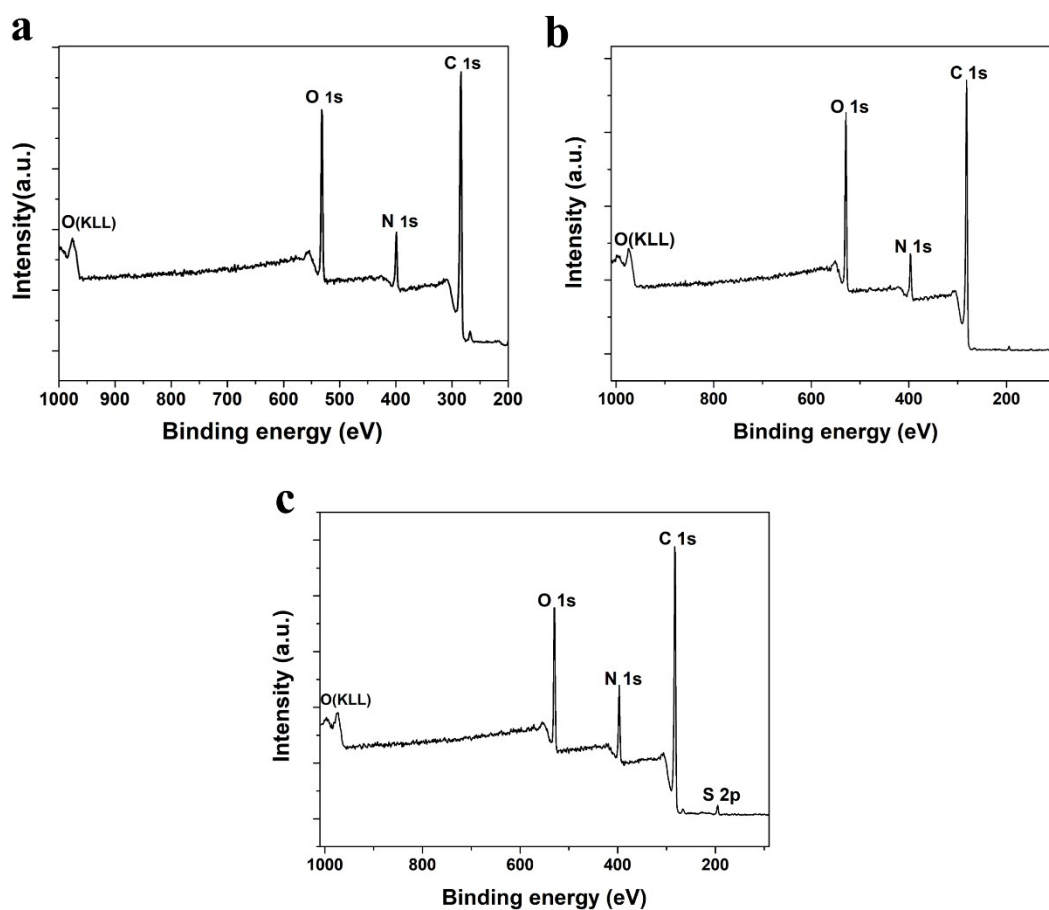
25 [3] D.K. Rope, W. Ahn, M. Hoepfner, J. Phys. Chem. C Nanomater. Interfaces, 2007, 111, 3636-  
26 3641.

1



2

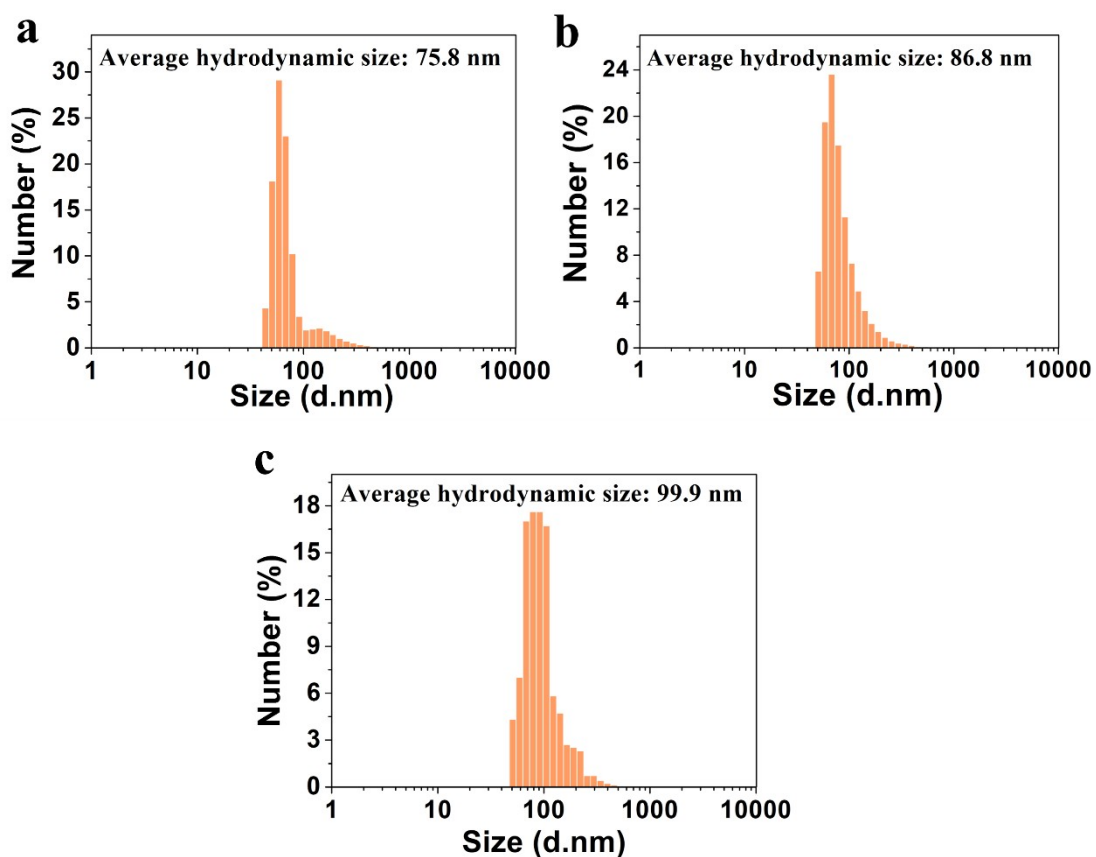
3 Figure S1. TEM images of PPy nanoparticles.



4

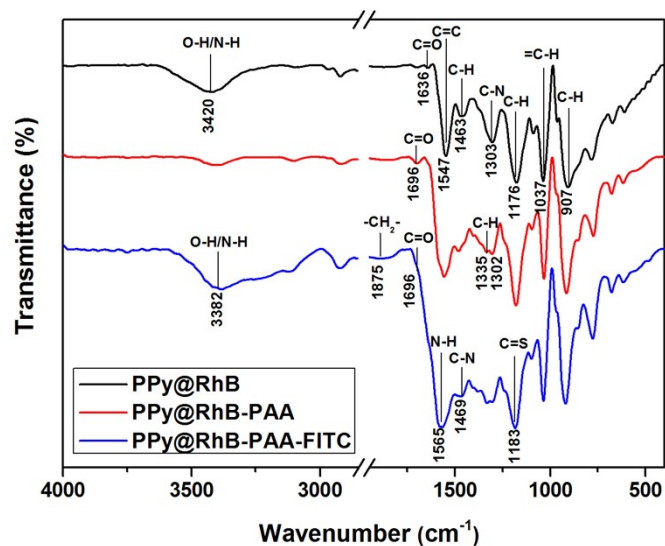
5 Figure S2. The XPS full scan spectra of (a) PPy nanoparticles, (b) PPy@RhB-PAA and (c)

6 PPy@RhB-PAA-FITC nanocomposites.



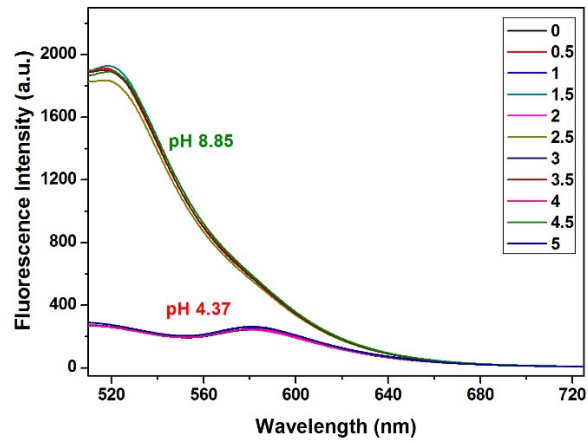
1

2 Figure S3. Size distributions of (a) PPy@RhB, (b) PPy@RhB-PAA and (c) PPy@RhB-PAA-FITC  
 3 nanocomposites by dynamic light scattering (DLS) tests.



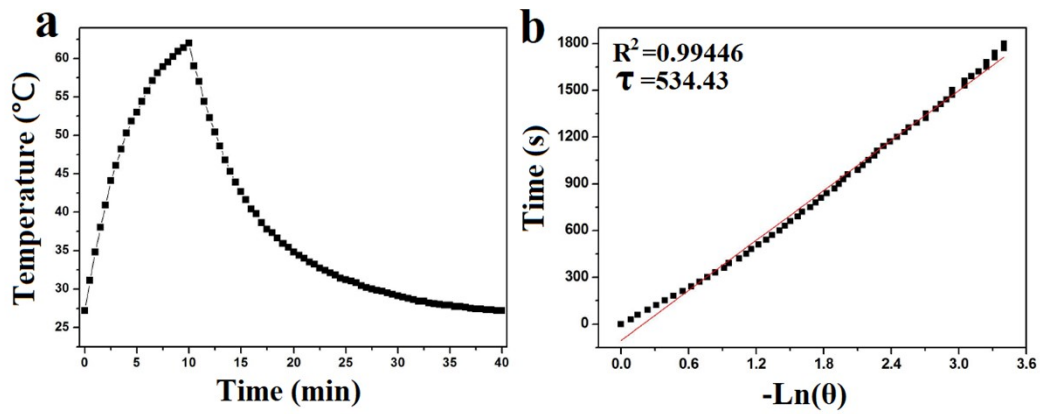
4

5 Figure S4. The FT-IR spectra of the obtained nanocomposites.



1

2 Figure S5. Reversible fluorescence spectra of PPy@RhB-PAA-FITC between pH 4.37 and 8.85.



3

4 Figure S6. Photothermal conversion efficiency curves of PPy@RhB-PAA-FITC nanocomposites.

5